1-12-2004

Accuracy limitations introduced by digital projection sources in profilometric optical metrology systems

Matthew J. Baker
matthewb@uow.edu.au

Joe F. Chicharo
University of Wollongong, chicharo@uow.edu.au

Jiangtao Xi
University of Wollongong, jiangtao@uow.edu.au

Enbang Li
University of Wollongong, enbang@uow.edu.au

Accuracy limitations introduced by digital projection sources in profilometric optical metrology systems

Abstract

The accuracy of profilometric optical metrology systems utilising Digital Fringe Projection (DFP) is analysed. An analytical model to describe theoretical accuracy limitation is derived and given as a function of object distance from the projector, projector resolution, projection angle and also object gradient. Associated limitations of the model are also discussed and analysed. The validity of the new model is demonstrated through practical experimentation.

Disciplines

Physical Sciences and Mathematics

Publication Details

This article was originally published as: Baker, MJ, Chicharo, JF, Xi, J & Li, E, Accuracy limitations introduced by digital projection sources in profilometric optical metrology systems, 2004 Conference on Optoelectronic and Microelectronic Materials and Devices, December 2004, 261-264. Copyright IEEE 2004.

Accuracy limitations introduced by digital projection sources in profilometric optical metrology systems.

Matthew J. Baker, Joe Chicharo, Jiangtao Xi and Enbang Li
School of Electrical, Computer and Telecommunications Engineering
University of Wollongong NSW 2522, Australia
Email: mjb06@uow.edu.au

Abstract— **The accuracy of profilometric optical metrology systems utilising Digital Fringe Projection (DFP) is analysed. An analytical model to describe theoretical accuracy limitation is derived and given as a function of object distance from the projector, projector resolution, projection angle and also object gradient. Associated limitations of the model are also discussed and analysed. The validity of the new model is demonstrated through practical experimentation.**

I. Introduction

Fast, high precision and automated optical noncontact surface profile and shape measurement has been an extensively studied research area due to its many potential applications in 3D sensing, industrial monitoring, mechanical engineering, medicine, robotics, machine vision, animation, virtual reality, dressmaking, prosthetics, ergonomics etc. One of the most promising techniques is fringe profilometry [1]–[5]. In fringe profilometry a fringe pattern composed of parallel lines is projected onto a diffuse surface to be measured and viewed from an offset angle. The observed fringe pattern is distorted by the object in such a way that represents information about the height of the object perpendicular to the plane of observation. The distorted fringe pattern is recorded, typically by a CCD camera and through computer analysis of the recorded image the object can be recreated in 3D space, generally with a high degree of precision.

In traditional profilometric optical metrology systems interferometric methods using a laser source are used to project the fringe pattern onto the object to be measured. An alternative to conventional laser projection is digital fringe projection (DFP). DFP is a technology which has been actively pursued by the research community because it provides a number of key advantages. For instance DFP provides the ability to manipulate fringe patterns easily with high precision in software, along with the capability to develop multi-channel algorithms [6]–[11] via colour fringe pattern projection. Advancements in performance of such digital technology in conjunction with these incentives have fueled continued interest from the research community over recent years, however, in contrast with the classic analogous laser source, the discrete nature of the digitally projected fringe pattern places a theoretical limit on the accuracy of the metrology system. This limitation was first discussed by Huntley and Saldner [12] in their analysis of temporal phase unwrapping, a technique well suited to DFP due to the associated flexibility in fringe map production.

Typical profilometry methods such as Fourier Transform Profilometry (FTP) and Phase Measuring Profilometry (PMP) can attain accuracies of $\lambda/100$ and $\lambda/1000$ [4], [13] corresponding to 10^{-5} m and 10^{-6} m respectively when a laser generated grating pattern with period in the order of millimeters is utilised (where λ is the fringe period). Conversely, when DFP is utilised the accuracy of the metrology system becomes a function of projector chracteristics and varies across the surface of the object being measured.

In this paper we review DFP fringe profilometry from an accuracy perspective discussing the standard height extraction technique utilised by all profilometry methods. The projection characteristics of a typical digital projector are analysed and hence for the first time according to our knowledge an analytical expression representing the theoretical limit of accuracy associated with DFP is derived. In our analysis we derive the projector pixel size and thus system accuracy as a function of object distance from the projector, projector resolution, projection angle and also object gradient. We have assumed the capture aspect associated with the accuracy of the system to be perfect and consequently define a theoretical limit that is considered approachable in practice. The proposed theoretical limit is validated through practical experimentation, the results confirm the usefulness of the analytical accuracy model.

II. A Review of DFP Fringe Profilometry

In DFP fringe profilometry the fringe or grating pattern projected onto the diffuse surface to be measured is created via a digital projection source. Common digital projection sources are typical video projectors generally either of Liquid Crystal Display (LCD) or Digital Light Processing (DLP, Texas Instruments) technology capable of projecting a standard 24 bit bitmap image [6]–[8], [10], [11]. Some recent work has also been performed utilising specialised projection sources projecting highly controlled grating patterns. Such specialised projection sources are capable of achieving very high accuracies down to the micron level, however, such solutions are quite expensive [14]. This work is primarily concerned with more typical projection sources namely DFP by way of

0-7803-8820-8/05/$20.00

video projection but is general enough to analyse any digital projection scheme.

Despite the digital projection technology used the projected fringe pattern results in a discrete-like intensity distribution that varies across the surface of the object in the form of pixels. Current video projector technology support resolutions from 640 x 480 up to approximately 1600 x 1200 pixels. Zhou and Liang [15] demonstrate the importance of captured intensity distribution and have shown its impact on the performance of profilometry sensing systems. In this paper we show that the discrete nature of the intensity distribution places a limitation on the accuracy of the system. This limitation becomes more apparent through analysis of the height extraction technique used by profilometry approaches.

A. Principle Profilometry Height Extraction

Well known profilometry methods such as FTP and PMP utilise similar optical arrangements, probably the most exploited optical arrangement is the Crossed Optical Axes geometry as seen in Figure 1 [3]. Projector and camera optical axes intersect at point O on reference plane R which is a fictitious plane normal to the camera optical axis and serves as a reference from which height *h(x,y)* is measured. Point D expresses a tested point on the diffuse object. Points B, A and C represent points on R, d_0 is the distance between E_p and E_c and l_0 is the distance between E_c and O. The *y*-axis is normal to the plane of the Figure (i.e. into the page) with the *x* and *z*-axes as indicated. Using geometrical relationships apparent in the arrangement the physical height distribution of the object can be extracted. Noting that $\triangle\ E_pE_cD$ and $\triangle\ ACD$ are similar it can be shown that

$$\frac{AC}{-h(x,y)} = \frac{d_0}{l_0 - h(x,y)}$$

$$h(x,y) = \frac{l_0 AC}{AC - d_0} \tag{1}$$

Close examination of Equation (1) reveals that the height resolution and hence system accuracy is dependent on three parameters, l_0, d_0 and spatial distance AC. Erroneous suppositions made about both l_0 and d_0 can be corrected when configuring the arrangement through specialised calibration algorithms [16], thus spatial distance AC can be considered the chief factor determining the accuracy of the system. Methods such as FTP and PMP determine spatial distance AC using phase analysis techniques which measure fringe pattern intensity [3], [4]. Since in DFP the intensity distribution of the projected signal is of a discrete nature this limits the precision to which AC can be measured and therefore limits the precision of the metrology system. We will now discuss the characteristics of the digitally projected intensity distribution.

B. Digital Projection Characteristics

As with any digital signal the digitally projected fringe pattern is sampled and quantised. The intensity distribution can be defined by pixels and each pixel is confined to a finite set of intensity values. When the signal is projected onto any diffuse surface the intensity distribution can be characterised primarily by the projection source, projection surface and the surface's distance from the projector. Aspects such as projector resolution, focus, projection angle, distance from the projector and object gradient can be used to mathematically describe the pixel deformation and hence intensity distribution. Since the spatial distance AC is determined through analysis of the intensity distribution of the projected fringe pattern, the ability to describe the intensity distribution mathematically provides the capability to describe system accuracy.

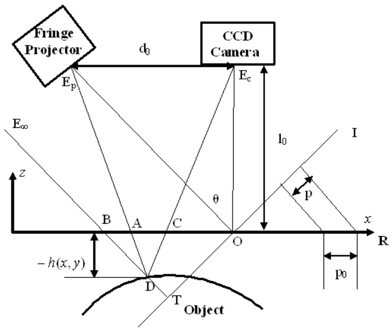

Fig. 1. Typical Crossed Optical Axes profilometry arrangement

Due to the fact that profilometry techniques utilise active triangulation this requires that the grating pattern be projected from an angle relative to the plane of observation and hence pixel deformation occurs over the entire projection field. Pixels vary in size and shape namely due to projection surface characteristics and surface's distance from the projector, and hence system accuracy varies accordingly. It should be noted that to calculate the height of the object at any one point we are only concerned with the distortion of the spatial distance AC in the x direction. Obviously pixels are distorted in both the x and y directions, however, only the distortion in the x direction is considered. The accuracy in the y direction can be analysed using similar ideas as presented here.

Since each pixel is quantised to a finite set of values care should be taken when selecting an appropriate fringe pattern frequency to ensure that no neighboring pixels are of identical intensity. To achieve maximum accuracy it can be shown that the frequency of the digital grating pattern should be chosen to be higher than the following condition to achieve maximum resolution.

$$f_{min} = 2^{no.bits+1}\ pixels\ per\ period \tag{2}$$

where *no.bits* refers to the number of bits used to quantise the intensity of the signal. Typical video projectors use an 8 bit RGB colour model to project standard bitmap images, thus, based on Equation (2) the period of the grating pattern for such a projector should be chosen to be less than 512 pixels.

III. Analysis

In order to analyse the digital projection characteristics of the optical subsystem some assumptions about the projection

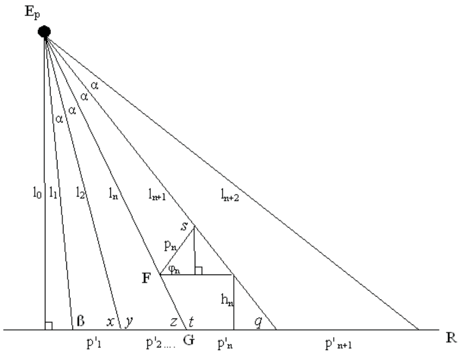

Fig. 2. Pixel projection characteristics

source and system features are made. In this analysis we assume that the projector is adequately focused over the range of interest, the angle subtended by any one pixel is the same, the gradient of the object is constant over the range of one pixel and that an appropriate frequency fringe pattern is selected as specified above. Figure 2 depicts a similar situation where E_p is the exit pupil of the digital projection source, α is the angle subtended by any one pixel, $p_n^{'}$ is the spatial size of the n^{th} pixel on the reference plane, l_n is the n^{th} pixel ray, β is the angle formed with the reference plane by the first pixel and defines projection angle, p_n is the spatial size of the n^{th} pixel based on h_n and ϕ_n, the average height and gradient of the object at the n^{th} pixel respectively. Figure 2 clearly demonstrates the deformation of pixels in the x direction and as a result the affect that will be incurred on the accuracy of the metrology system across the full field of projection.

Given the stated assumptions one can derive an analytical model to describe pixel size and hence system accuracy. Using some applied geometry together with the sine rule it can be shown that the size of the n^{th} pixel in the x direction can be given as follows:

$$p_n = \left[\frac{\left(l_n - \frac{h_n}{\cos(\beta + (n-1)\alpha - \pi/2)} \right) \sin(\alpha)}{\sin(\pi - \beta - (\alpha n - \phi_n))} \right] \cos(\phi_n) \quad (3)$$

where

$$l_n = \frac{l_{n-1} \sin(\beta + (n-2)\alpha)}{\sin(\pi - \beta - (n-1)\alpha)} \quad for\, n = 2 \rightarrow res$$

$$l_1 = \frac{l_0}{\sin(\pi - \beta)}$$

where *res* refers to the the resolution of the digital projector in the x direction.

A. Model Limitations

Due to the nature of the assumptions made in deriving the accuracy model, constraints are placed on the precision in which the accuracy can be determined. The two most confining assumptions made in this analysis are that the height and gradient of the object at any one pixel are restricted to a single finite value. Obviously, this assumption will be more appropriate for specific objects with constant height and gradient over the space of one pixel, however, in general will not be suitable and hence this limitation should be further explored. Figure 3 clearly demonstrates pixel size as a function of height where p^{hn} is the height of the n^{th} pixel at some arbitrary height h_n. It should be noted that maximum variation in pixel size occurs when the gradient is zero so we consider this case only. Under the assumed conditions it can be shown that pixel size is a linear function of height and hence, x meters deviation in the z direction corresponds to a specific amount of deviation in the x direction. Considering this it becomes clear that a restriction is enforced on the gradient if the accuracy is to be calculated within some specified precision. Evidently, accuracy will be an application-specific attribute of the system and varies accordingly with geometrical arrangement thus a tolerated range of precision should be decided a priori. In this analysis we suggest a more generic limitation, this height limitation is given as a percentage of pixel size as follows

$$\Delta h_{max} = \frac{p^{hn}}{p'^{n}} \quad (4)$$

where Δh_{max} is the maximum acceptable height deviation. A value of 0.95 could be chosen for example if the accuracy is to be determined within 5% of a pixel. With this specified accuracy tolerance in place the gradient limitations can be defined by the following two equations.

$$\phi_{+ve} = \arctan\left(\frac{|p_1 - \Delta h_{max} \tan(\beta - \pi/2)|}{\Delta h_{max}} \right) + \pi/2 \quad (5)$$

and

$$\phi_{-ve} = \arctan\left(\frac{\Delta h_{max}}{\Delta h_{max} \tan(\pi/2 - (\pi - (\beta + \alpha res)) + p_{res})} \right) \quad (6)$$

where ϕ_{+ve} and ϕ_{-ve} refer to the positive and negative gradient limits respectively. The following section verifies the usefulness of the analytical model through experiment.

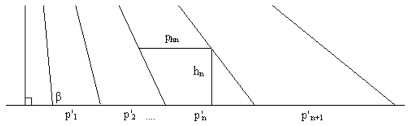

Fig. 3. Pixel size variation with height

IV. Experimentation

In order to demonstrate the performance of the analytical model, practical experimental results were established to measure the size of projected pixels. The experiment utilised an optical arrangement similar to that as seen in Figure 1 to project a Ronchi grating onto a flat surface that served as a reference plane. The plane corresponded to an object with a uniform height distribution and gradient of 0. Each fringe of the bitmap grating was exactly 10 pixels in width with

the intensity varying white (255,255,255) to black (0,0,0). The Ronchi distribution was projected using an InFocus LP530 DLP projector 1024 by 768 pixels. The grating pattern was captured using a high resolution CCD camera, from the captured intensity distribution pixel size was calculated based on fringe widths. System parameters β, α and l_0 were measured as 1.713 rads, 0.00536 rads and 1.959 m respectively to be within 0.08% accuracy. Using these parameters the predicted values for pixel size as determined by means of the analytical model could be ascertained. The fringe width and hence pixel size was determined by measuring the number of camera pixels contained within the fringe of interest. A simple calibration factor accurate down to 6.44 x 10^{-5} m was introduced to convert the measurement from pixels into meters. Figure 4 displays both the experimental and simulated results for fringe size in the x direction, with the experimental data represented by + and the simulated data as produced using the model represented by the solid line. The peak relative error measured was 1.3166% with an average relative error of 0.4208%.

Close examination of Figure 4 indicates that the distribution of the experimental results closely imitates that of the analytical data. Experimental results were found to be within experimental error with an absolute average error of 5.021 x 10^{-5} m when taking into consideration the calibration factor. The observable errors do not appear systematic but rather more randomly distributed in nature. This is namely due to the subjectivity introduced into the fringe edge determination algorithm. Fringe edges were determined based on intensity values, if the intensity value fell into a predefined threshold it was consider the edge of a fringe. Two underlying factors introduced such errors; intensity fluctuations due to the projector and focusing of the projector. The latter proved to influence results more so than the former as the projector had to be continually refocused as multiple shots of the intensity distribution were taken as a result of projecting from an angle. Consequently this introduced human error as focusing was performed visually. Intensity fluctuations were inherent in this experimentation due to DLP projection technology utilised. DLP projectors project multiple images of different intensities at high speed and hence without synchronisation of the camera and projector this introduced minor errors as threshold values had to be shifted accordingly. In future work synchronisation of camera and projector and also a more efficient solution to adequately focusing the projector will be considered.

V. Conclusion

The accuracy limitations involving digital projection sources in optical profilometry arrangements has been demonstrated. An analytical model and associated limitations to describe the accuracy of such a system has been proposed and verified. With more and more industrial applications utlising digital technology in profilometric sensing such limitations as presented in this paper should be of significant value and practical use.

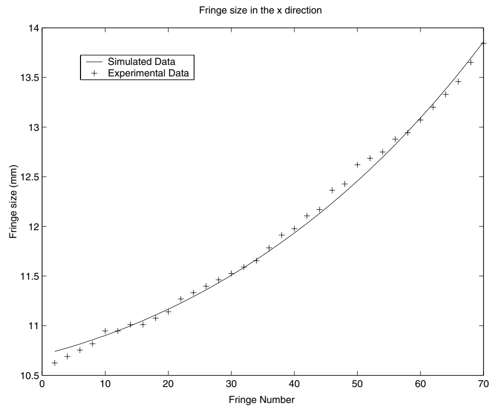

Fig. 4. Fringe Size in the x direction

References

[1] F. Chen, G. M. Brown, M. Song, "Overview of three-dimensional shape measurement using optical methods," *Optical Engineering*, vol. 39, pp. 10–22, January 2000.

[2] X. Su, W. Chen, "Fourier transform profilometry: a review," *Optics and Lasers in Engineering*, vol. 35, pp. 263–284, 2001.

[3] M. Takeda, K. Mutoh, "Fourier transform profilometry for the automatic measurement of 3-d object shapes," *Applied Optics*, vol. 22, pp. 3977–3982, December 1983.

[4] V. Srinivasan, H. C. Lui, M. Halioua, "Automated phase-measuring profilometry of 3-d diffuse objects," *Applied Optics*, vol. 23, pp. 3105–3108, 1984.

[5] V. Srinivasan, H. C. Lui, M. Halioua, "Automated phase-measuring profilometry: a phase mapping approach," *Applied Optics*, vol. 24, pp. 185–188, January 1985.

[6] L. Kinell, "Multichannel method for absolute shape measurement using projected fringes," *Optics and Lasers in Engineering*, vol. 41, pp. 57–71, 2004.

[7] L. Kinell, M. Sjodahl, "Robustness of reduced temporal phase unwrapping in the measurement of shape," *Applied Optics*, vol. 40, no. 14, pp. 2297–2303, May 2001.

[8] P. S. Huang, Q. Hu, F. Jin, F. Chiang, "Color-encoded digital fringe projection technique for high speed three-dimensional surface contouring," *Optical Engineering*, vol. 38, pp. 1065–1071, 1999.

[9] W. Liu, Z. Wang, G. Mu, Z. Fang, "A novel profilometry with color-coded project grating and its application in 3d reconstruction," vol. 2, Fifth Asia-Pacific Conference on Communications and Fourth Optoelectronic and Communications Conference. IEEE Explore, October 1999, pp. 1039–1042.

[10] O. A. Skydan, M. J. Lalor, D. R. Burton, "Technique for phase measurement and surface reconstruction by use of colored structured light," *Applied Optics*, vol. 41, no. 29, pp. 6104–6117, October 2002.

[11] P. S. Huang, C. Zhang, F. Chiang, "High-speed 3-d shape measurement based on digital fringe projection," *Optical Engineering*, vol. 42, no. 1, pp. 163–168, January 2003.

[12] J. M. Huntley, H. O. Saldner, "Error-reduction methods for shape measurement by temporal phase unwrapping," *Journal of the Optics Society America*, vol. 14, no. 12, pp. 3188–3196, December 1997.

[13] M. Kujawinska, J. Wojciak, "High accuracy fourier transform fringe pattern analysis," *Optics and Lasers in Engineering*, vol. 14, pp. 325–339, 1991.

[14] W. Su, H. Liu, K. Reichard, S. Yin, F T. S. Yu, "Fabrication of digital sinusoidal gratings and precisely controlled diffusive flats and their application to highly accurate projected fringe profilometry," *Optical Engineering*, vol. 42, pp. 1730–1740, June 2003.

[15] J. Zhou, Z. Liang, "Several factors impairing the phase measurement accuracy," *Optics and Lasers in Engineering*, vol. 23, pp. 199–212, 1995.

[16] W. S. Zhou, X. Y. Su, "A direct mapping algorithm for phase-measuring profilometry," *Journal of Modern Optics*, vol. 41, pp. 89–94, 1994.